Carbohydrate Polymers 145 (2016) 121–131

Contents lists available at ScienceDirect

Carbohydrate Polymers

journal homepage: www.elsevier.com/locate/carbpol

Synthesis and characterization of photo-crosslinkable 4-styryl-pyridine modified alginate

Nadia H. Elsayed[a,b], M. Monier[c,*], Raedah A.S. Alatawi[a]

[a] Department of Chemistry, Faculty of Science, University of Tabuk, Tabuk 71421, Saudi Arabia
[b] Department of Polymers and Pigments, NRC, Dokki, Cairo 12311, Egypt
[c] Chemistry Department, Faculty of Science, Mansoura University, 35516 Mansoura, Egypt

ARTICLE INFO

Article history:
Received 12 December 2015
Received in revised form 2 March 2016
Accepted 3 March 2016
Available online 5 March 2016

Keywords:
Alginate
Styryl-pyridine
Photo-crosslinking
Cycloaddition

ABSTRACT

In this article photo-crosslinkablestyryl-pyridine modified alginate (ASP-Alg) was prepared and entirely investigated utilizing different instrumental techniques such as Elemental analysis, Fourier transform infrared (FTIR),^{13}C and ^{1}H nuclear magnetic resonance (NMR), ultraviolet-visible light (UV-vis), X-ray diffraction (XRD) spectra and scanning electron microscope (SEM). Upon irradiation in the UV region, the casted ASP-Alg membranes were cross-linked through the [2π + 2π] cycloaddition reaction of the inserted photo-active styryl pyridine moieties. Both cross-linking density and kinetics were monitored by examining the UV–vis light spectra of the irradiated membrane at predetermined time intervals and the obtained results were found to fit with the second order mathematical kinetic model, revealing the performance of the cross-linking via bimolecular [2π + 2π] cycloaddition reaction. Also, the swelling behaviors along with biodegradability were also studied, and the results indicated the decrease of the swelling ratio and degradation rate by increasing the cross-linking density. Moreover, the mechanical properties were also examined under both wet and dry conditions.

1. Introduction

Alginate is a natural carbohydrate that mainly extracted from brown algae as a copolymer containing both β-D-mannuronate (M) and α-L-guluronate (G) units in block pattern *i.e.* MMM-GGG or alternating pattern *i.e.* MGMGM (Chiang & Chu, 2015; Bruchet & Melman, 2015; García-González, Alnaief, & Smirnova, 2011; Gong et al., 2011; Goh, Heng, & Chan, 2012). Due to the presence of the carboxyl functional groups within these monomeric sugar unites, algenate are able to bind with di or tri valent metal ions such as Ca^{2+} or Al^{3+} to create ionically cross-linked network structures (Jang et al., 2014; Monier, Abdel-Latif, & Mohammed, 2015). Upon treatment with Ca^{2+}, the cross-linked alginate hydrogel is formed by aggregation of the carboxylate groups, which exist mainly in the GG units resulting in egg-box formatting structure (Graulus et al., 2015). Because of its high biocompatible and non-immunogenic properties (Bubenikova et al., 2012), ionically cross-linked alginate hydrogels had been employed in various pharmaceutical and biomedical applications such as drug delivery systems (Yang, Shi, Zhou, & Shaokui Cao, 2015; Agarwal et al., 2015; Wu, Wang, Zhuo, & Cheng, 2014), wound dressing (Peng, Lin, Wang, & Wu, 2012; Han, Dong, Song, Yin, & Li, 2014; Sweeney, Miraftab, & Collyer, 2014), tissue engineering (Qiao et al., 2013; Tang, Chen, Weir, Thein-Han, & Xu, 2012; Lee, Park, Shin, & Kim, 2011), enzymes and cell immobilization (Dong, Zhang, Tu, & Miao, 2014; Abd Rahima et al., 2013; Abd El-Ghaffar & Hashem, 2013; Wang, Chen, Wang, & Xing, 2014) etc. However, the difficulty to control the ionicgelation mechanism in addition to the formation of heterogeneous network structure could sometimes limit its application in these biomedical areas (Bruchet & Melman, 2015).

In order to overcome the drawbacks of the ionic cross-linking technique, various attempts were made to prepare covalently cross-linked alginate based hydrogels such as De Santis, Diociaiuti, Cametti, and Masci (2014) where alginate and Hyaluronic acid were cross-linked using l-lysine ethyl ester, Stone, Gosavi, Athauda, and Ozer (2013) where alginate/polyvinyl alcohol were cross-linked using citric acid and Mandal & Ray (2013) who cross-linked alginate in presence of acrylic acid (AA) and hydroxy ethyl methacrylate in aqueous solution. Despite the efficiency of these methods in minimizing the disadvantages of the ionic cross-linking, the use of some reagents such as initiators in addition to the formation of unfavorable and sometimes toxic products during the biodegradation still

* Corresponding author.
E-mail addresses: nhussein@ut.edu.sa (N.H. Elsayed), monierchem@yahoo.com (M. Monier).

http://dx.doi.org/10.1016/j.carbpol.2016.03.006
0144-8617/

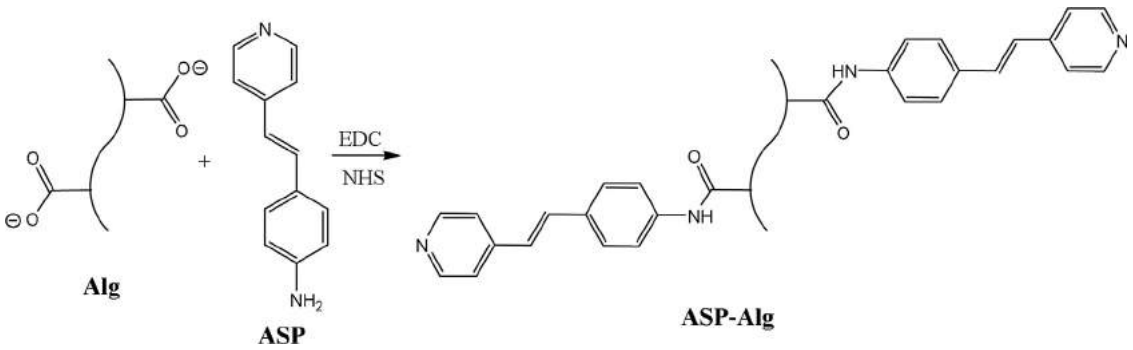

Scheme 1. Synthesis of ASP-Alg.

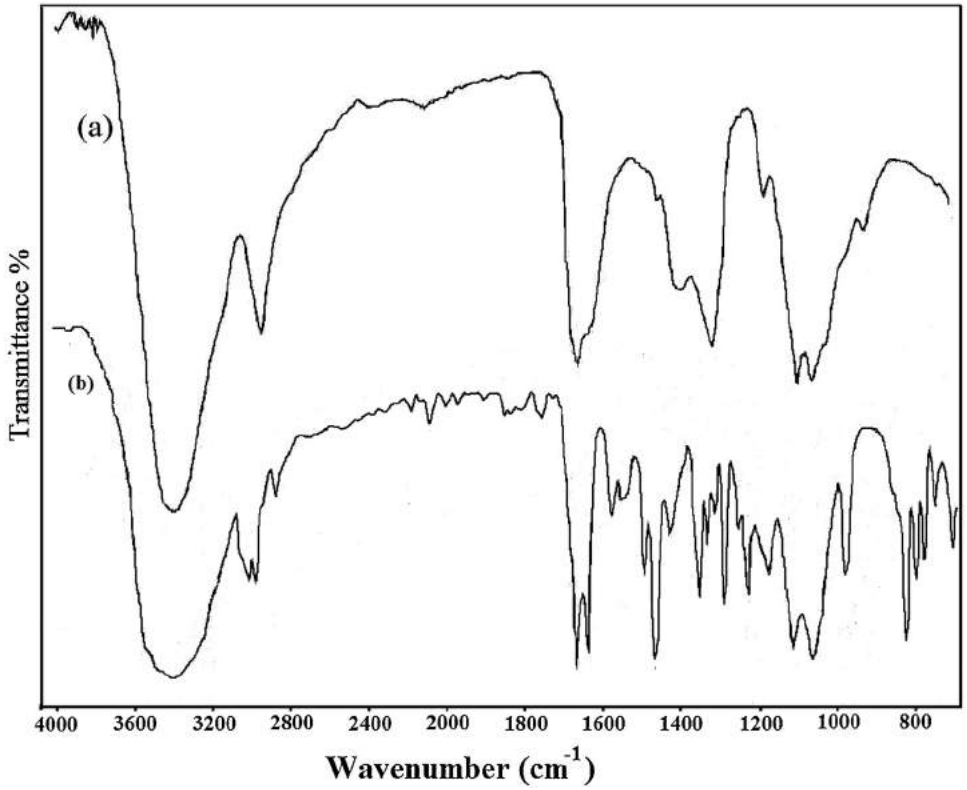

Fig. 1. FTIR spectra of (a) Alg and (b) ASP-Alg-2.

a serious drawback, which could still limits the pharmaceutical and biomedical application.

In this work, photo-crosslinkable alginate functionalized with styrylpyridine (ASP-Alg) had been synthesized and investigated utilizing Elemental analysis. Fourier transform infrared (FTIR), nuclear magnetic resonance (^{13}C and ^{1}HNMR) wide angle X-ray diffraction (XRD) spectra in addition to scanning electron microscope (SEM). The initiator-free photo-crosslinking process had been carried out by UV irradiation, through the [2π + 2π] cycloaddition reaction of the inserted photo-active styryl pyridine moieties. Both extent and kinetics of the photo-crosslinking were monitored by UV–vis light spectra.

2. Materials and methods

2.1. Materials

Sodium alginate (Alg) ($M_w = 2 \times 10^5$ Da and viscosity 735 cps at 25 °C) was purchased from Alfa Aesar (USA) and used without further purification. The G/M ratio was determined by NMR to be 6.8. 1-Ethyl-(dimethylaminoprolpyl) carbodiimide (EDC) and *N*-hydroxysuccinimide (NHS) were also obtained from Alfa Aesar (USA). Trans-4-[*p*-(amino)styryl]pyridine (ASP) was supplied from Hangzhou Chempro Tech Co. (China). All other chemicals and solvents were of analytical grade and used as provided.

2.2. Synthesis of photo-crosslinkablestyrylpyridine-alginate (ASP-Alg)

The chemical modification of the alginate was performed by insertion of the photo-active (ASP) moieties through the amide bond formation between the Alg carboxyl and the ASP amino groups in presence EDC/NHS combined coupling agent as presented in Scheme 1. The formulation codes are collected in Table 1. Briefly, 0.5 g Alg was dissolved in 50 mL distilled water to get clear solution. Then a mixture of 0.14 g NHS and 1.16 g EDC was charged into the reaction flask and the mixture was magnetically stirred until homogeneous solution was obtained. In separate vials, aque-

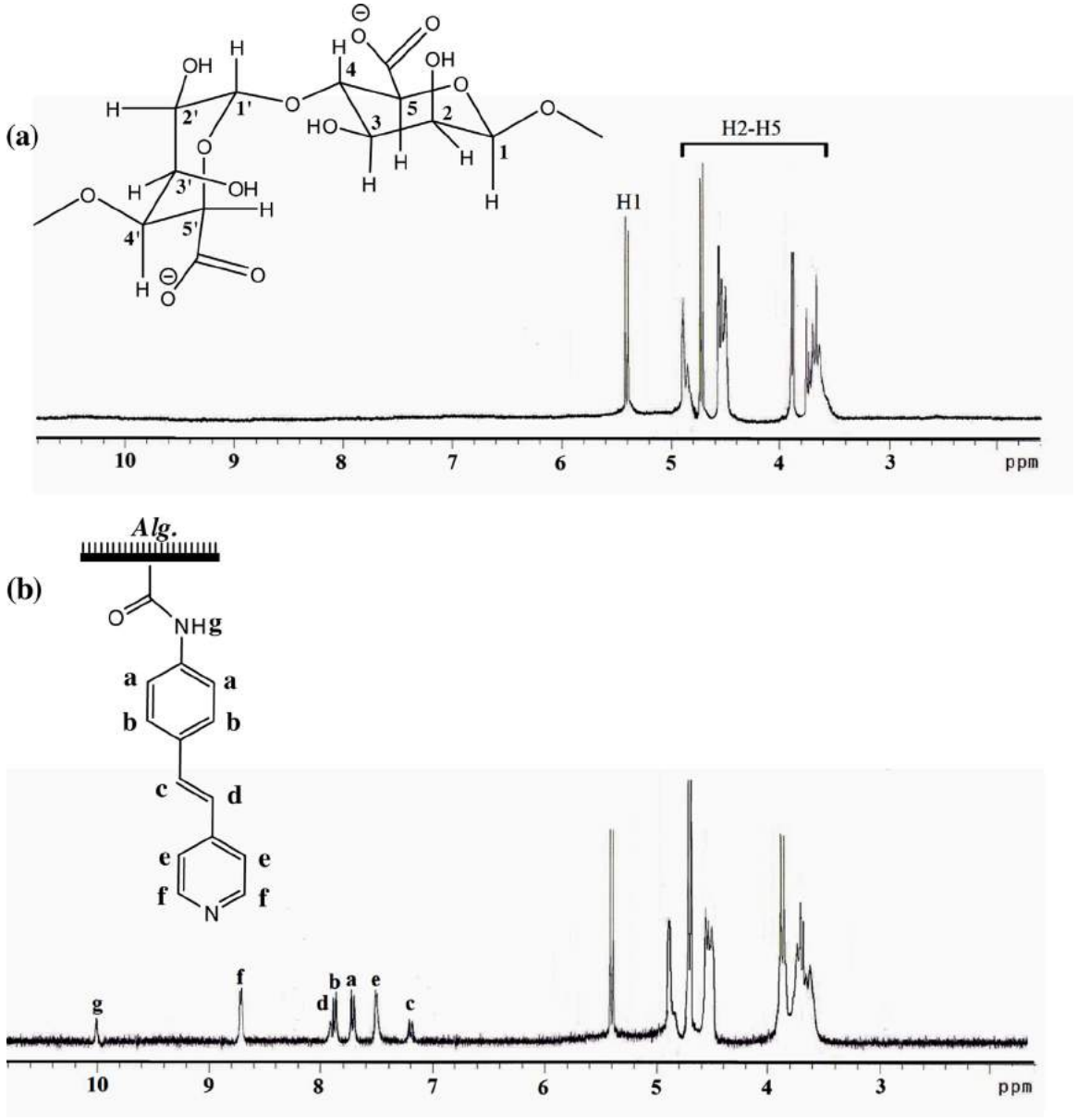

Fig. 2. ^{1}H NMR spectra of (a) Alg and (b) ASP-Alg-2 with D_2O as solvent.

Table 1
Synthesis of ASP-Alg using EDC/NHS conjugation method[a].

Formulation code	ASP (mol/L)	DS[b] (mol %)
ASP-Alg-1	0.03	25%
ASP-Alg-2	0.06	41%
ASP-Alg-3	0.09	68%

[a] Concentration of Alg solution = 10 g/L; reaction time: 24 h at room temperature.
[b] Degree of ASP substitution (DS) determined by ^{1}HNMR, DS (mol%) = I_g/I_1, where I_g denote the integral of the amide—NH-peak of the inserted ASP units, and I_1 denotes the integral of the peak of the proton H_1 in C-1 of the Alg.

Table 2
Elemental analysis of modified and unmodified alginate samples.

Sample	C(%)	H(%)	N(%)	DS(%)
Alg	37.6	4.2	0.003	–
ASP-Alg-1	46.9	4.6	3.01	23.6
ASP-Alg-2	55.7	5.02	5.2	44.2
ASP-Alg-3	60.2	5.1	6.7	70.5

ous ASP solutions were prepared by dissolving specific amounts in diluted HCl, which were then injected into the reaction mixture and stirring continued for 24 h in dark at room temperature. The modified ASP-Alg was precipitated by adding excess amount of acetone then filtered, washed with ethanol and finally dried at 40 °C in dark. The extent of ASP functionalization was evaluated utilizing ^{1}HNMR spectra and the obtained samples with substitution degrees (DS) 25%, 41% and 68% were respectively named ASP-Alg-1, ASP-Alg-2 and ASP-Alg-3.

2.3. Photo-crosslinking of ASP-Alg

0.5 g of the previously prepared ASP-Alg with various DS values was dissolved in 20 mL distilled water then the solution was poured in 5 cm diameter Petri dish and left to dry in dark overnight under vacuum at 40 °C. The obtained dry thin membranes with approximate thickness 0.2 mm were then sandwiched between two quartz slides and UV irradiated using high pressure 200W mercury UV

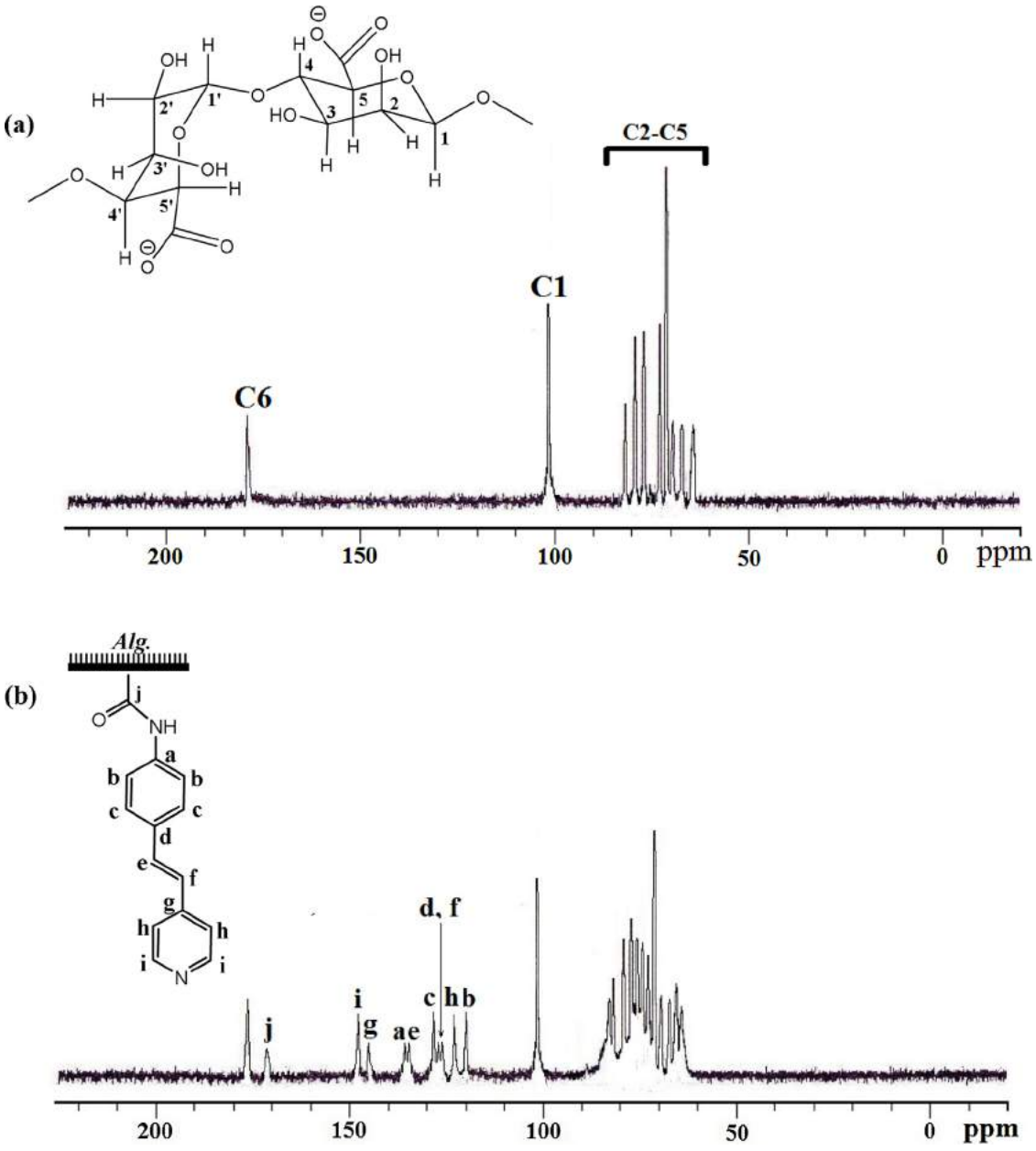

Fig. 3. ^{13}C NMR spectra of (a) Alg and (b) ASP-Alg-2 with D_2O as solvent.

lamp at 360 nm. The UV–vis spectra were then recorded upon irradiation for predetermined periods of time in order to hit upon the progress and kinetics of the photo-reaction.

At any time, the density of the photo-crosslinking (ρ_t) was estimated using Eq. (1) (Tie et al., 2012).

$$\rho_t = \frac{A_0 - A_t}{A_0} \times 100 \quad (1)$$

where A_0 is the initial absorbance intensity and A_t is the absorbance at time t.

2.4. Biodegradation studies

The biodegradation experiments were carried out in simulated body fluid (SBF) composed of a mixture of NaCl, $NaHCO_3$, KCl, $K_2HPO_4{\cdot}3H_2O$, $MgCl_2{\cdot}6H_2O$, HCl, $CaCl_2$ and $(CH_2OH)_3CNH_2$, which prepared according to a previous report (Pereira, Carvalho, Gil, Mendes, & Bártolo, 2013). After 60 min UV irradiation, the photo-crosslinked membranes that derived from ASP-Alg-1, SP-Alg-2 and SP-Alg-3 were cut into approximately regular rectangular pieces (5 mm × 10 mm) and incubated with SBF containing alginate lyase enzyme (10 U/g ASP-Alg) at pH 7.4 and 37 °C with renewed medium each 48 h. After predetermined time intervals, the swelled membrane sample was removed, washed with distilled water and dried at 37 °C. The extent of the enzymatic biodegradation was estimated by evaluating the weight loss according to Eq. (2).

$$\text{Weight loss}\,(\%) = \frac{W_i - W_t}{W_i} \times 100 \quad (2)$$

where W_i is the initial membrane weight and W_t is the membrane weight after incubation time t.

For hydrolytic degradation studies, the above experiments were also performed but using enzyme free SBF solution. In all cases, the average result of three performed samples was taken as a final reading for each point.

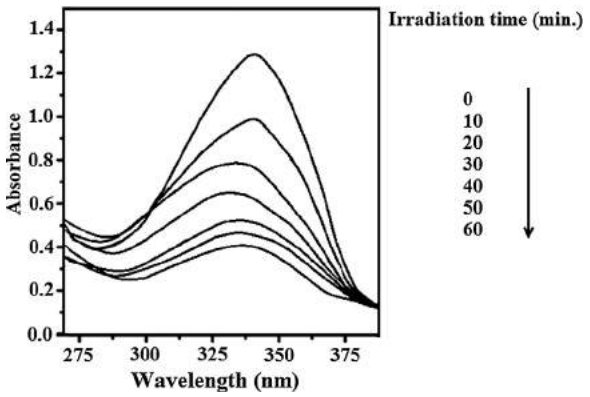

Fig. 4. Changes in the UV spectral patterns of ASP-Alg-2 membrane after UVirradiation time t = 0, 10, 20, 30, 40, 50 and 60 min.

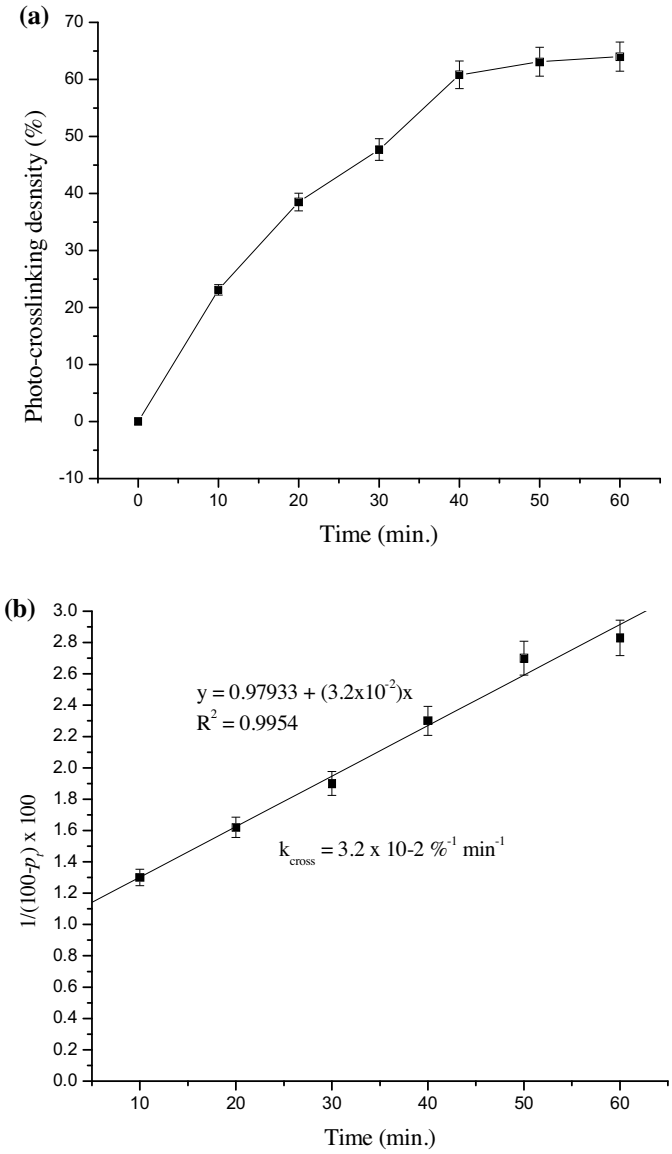

Fig. 5. (a) The effect of irradiation time on thephoto cross-linking density of ASP-Alg-2 (b) Linear second order integral plot of the reciprocal of the percentage of theuncross-linking against the time.

2.5. Swelling studies

The swelling studies were performed by immersing the previously weighed membrane pieces into pH pre-adjusted solution for 3 h to assure that the equilibrium swelling had been reached. The membranes were then withdrawn on a dry filter paper to remove the unabsorbed water and weighed. The swelling ratio (SR) was then calculated using Eq. (3).

$$\text{Swelling Ratio (SR)} = \frac{W_{wet} - W_{dry}}{W_{dry}} \times 100 \quad (3)$$

where W_{dry} and W_{wet} are the weights of the studied membrane before and after the swelling respectively.

2.6. Instrumentation

Elemental analysis examinations of the polymeric materials before and after modification had been performed utilizing PerkinElmer 240C Elemental Analytical Instrument (USA). Fourier transform infrared spectra (FTIR) were obtained using a PerkinElmer instrument supported with ATR.^{1}H and ^{13}C NMR spectra were performed on Oxford NMR instrument (Model Unity Inova 500 MHz, USA) using 3-(trimethylsilyl) propionic-2,2,3,3-d4 acid (Sigma) as an internal standard.

The degree of the photo-crosslinking was monitored using PerkinElmer Bio UV–vis spectrophotometer. X-ray diffraction (XRD) spectra of Alg and ASP-Alg-2 before and after photocrosslinking were investigated using X-ray powder diffractometer (Japanese Dmax-rA, wavelength = 1.54 A›, CuKα radiation). The samples were scanned from 2θ = 5–50° at a scan speed of 1.2° min^{-1}, in step of 0.02° using generator intensity of 40 kV and generator current of 50 mA. Scanning electron microscope (SEM) photos were taken using FEI Quanta-200 scanning electron microscope (1 kV, aperture: 15 μm, magnitude 100× −20 k×) (FEI Company, The Netherlands). The membranes were swelled in deionized water for 24 h then freeze–dried prior to the SEM morphological examination.

For mechanical properties measurements, the polymeric membranes with various cross-linking degrees were cut into regular 50 mm × 15 mm strips with approximate 0.2 mm thickness. The tensile strength and elongation was estimated utilizing Lloyd universal testing machine (model LR5 K, UK) supplied with vernier calipers. Under both wet and dry conditions, the measurements were performed eight times and after neglecting the maximum and minimum values, the average of the other six points was taken.

3. Results and discussion

3.1. Sample characterization

The prepared polymeric materials were investigated by elemental analysis and the obtained data were collected in Table 2. The appearance of nitrogen with incremental percentage, gives an evidence for the insertion of the ASP units onto the Alg backbone. The DS values were also estimated to compare with that from the NMR spectra.

The FTIR spectrum of the native Alg (Fig. 1a) displayed the diagnostic alginate peak at 3000–3600 cm^{-1}, which is related to the O—H bond stretching vibration in addition to the peaks at 1650 and 1460 cm^{-1} due to the asymmetric and symmetric carboxylate vibration, respectively (Daemi & Barikani, 2012). Furthermore, the spectrum of the modified ASP-Alg-2 (Fig. 1b) showed indicative peaks at 1661 cm^{-1} and 1587 cm^{-1}, which are related to the C=O and C—N of the formed amide (—CO—NH—) linkage and the peaks at approximately 3000, 1410 and 1450 cm^{-1}, which are respectively related to C—H, C=C and C=N of the pyridine ring in addition to the

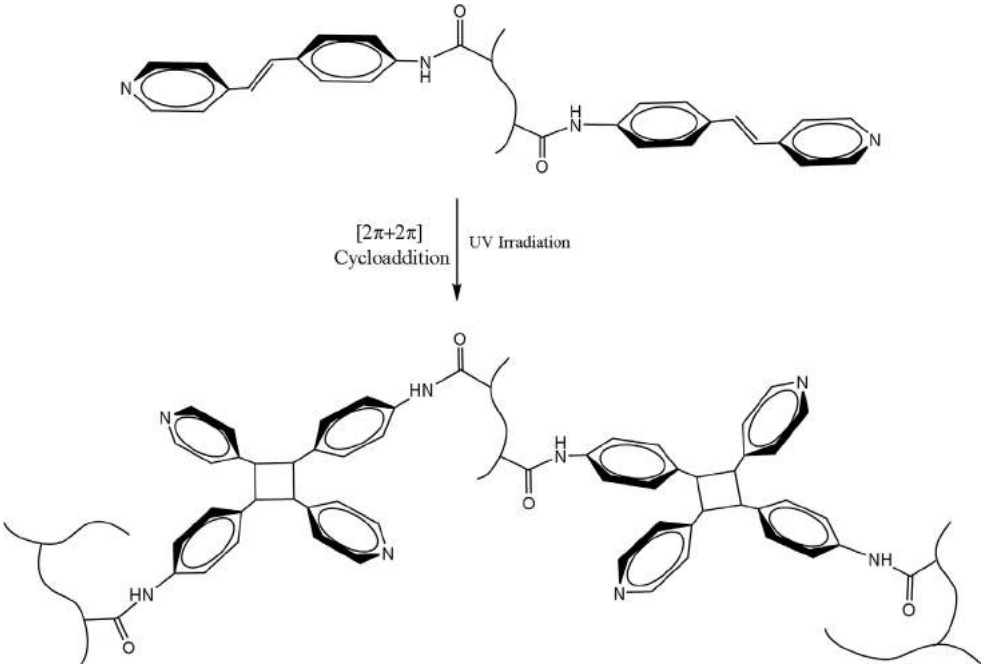

Scheme 2. Photo-crosslinking of ASP-Alg.

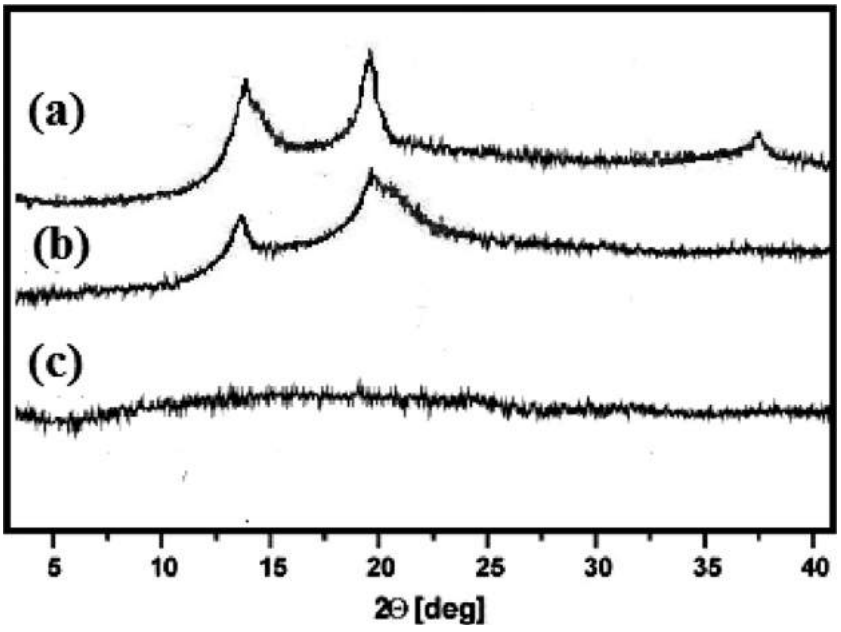

Fig. 6. XRD patterns of (a) Alg, (b) uncrosslinked ASP-Alg-2, and (c) photocrosslinked ASP-Alg-2.

peak at about 1570 cm^{-1} that correspond to the C=C of the phenyl ring. These results were in accordance with previous report (Castro et al., 2013).

The ^{1}H NMR spectra of Alg and ASP-Alg-2 were presented in Fig. 2. As previously reported (Bubenikova et al., 2012; Laurienzo, Malinconico, Motta, & Vicinanza, 2005; Pluemsab, Sakairi, & Furuike, 2005) beside the complex overlapped signals, the spectrum of the native Alg (Fig. 2a) displayed characteristic essential signals at 5.46 ppm, which correspond to H1 of guluronic units, 5.06, which is related to both H1 of the mannuronic acid units and H5 of mannuronic adjacent to glucouronic units in addition to 4.87 ppm, which assigned to H5 of the glucouronic attached to glucouronic units. On the other hand, the spectrum of ASP-Alg-2 (Fig. 2b) confirmed the ASP alginate modification by the appearance of the doublet aromatic signals at 6.31, 7.66 ppm, which are related to the *p*-disubstituted benzene ring, doublet signals at 7.20, 7.91 ppm, which are assigned for the trans H-atoms around the C=C, in addition to the doublet signals at 7.53, 8.72 ppm due to the aromatic pyridine ring. These signals were in a great agreement with that previously reported (Nakamura, Irie, Hara, Sugawara, & Yamada, 2011). The DS values were estimated by comparing the integration of the inserted ASP protons to that of glucouronic H1 at 5.46 ppm.

Moreover, ^{13}C NMR (125 MHz) spectra were also employed to confirm the reaction performance. As can be seen in Fig. 3, the characteristic ASP signals at 114.1, 122.5, 129.6 and 147.6 ppm cor-

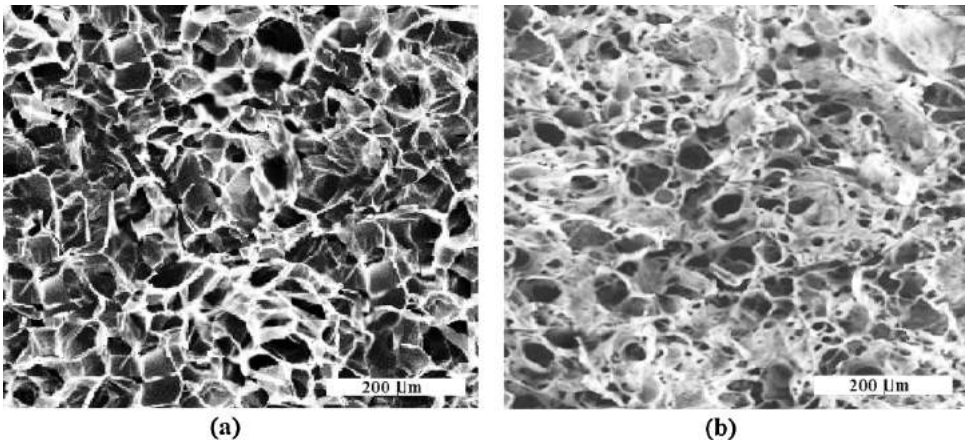

Fig. 7. SEM images of a cross-section of photo-crosslinked hydrogel membrane derived from (a) ASP-Alg-1 and (b) ASP-Alg-3.

respond to the benzene, at 127.1 and 134 ppm, which are assigned for C=C, and at 123.0 and 149.6 ppm that related to the pyridine ring confirmed the successful interaction between Alg and ASP.

3.2. Photo-crosslinking reaction

The photo-induced cross-linking of the modified ASP-Alg was carried out by exposing the casted thin membranes to the UV irradiation, which induces the concerted [2π + 2π] cycloaddition reaction between the inserted photo-active ASP units to obtain cyclobutane junctions that link the polysaccharide chains in three dimensional cross-linked network structure as shown in Scheme 2. The progress of the reaction was detected by examining the UV–vis light spectra of the irradiated membrane after predetermined time intervals. As can be seen in Fig. 4, the main characteristic ASP band at approximately 340 nm exhibited an obvious intensity decrease by increasing the irradiation time, which may reveal the involvement of these inserted moieties in the photo-induced cross-linking reaction.

In order to account for the reaction kinetics, the cross-linking density was estimated and plotted against the UV irradiation time (Fig. 5a). Moreover, the integral method was utilized to evaluate the most appropriate kinetic model, which describes the obtained kinetic data. The second order kinetic model (Eq. (4)) (Zhu, Kustra, & Bettinger, 2013) was found to be the most suitable model that fit with the obtained results; this was clarified by the linear relationship obtained by plotting the reciprocal of the uncross-linking percentage ($1/100-\rho_t$) against time t (Fig. 5b). These results reveal that the cross-linking reaction was performed via [2π + 2π] second order reaction with rate constant 3.2×10^{-2} $\%^{-1}$ min^{-1}.

$$\frac{1}{A} = \frac{1}{A_0} + kt \quad (4)$$

The molecular modeling was carried out using HyperChem software version 8.03 in order to optimize the geometry of the photo-crosslinkable units before and after the reaction performance. The most stable conformation presented in Structure 1a indicated that the ASP moieties are apart from each other, which minimize the steric problems during the chain approach and enhance the progress of the intermolecular [2π + 2π] cycloaddition reaction as displayed in Structure 1b.

3.3. Characterization of the photo-crosslinked ASP-Alg

The crystalline structures of the modified alginate samples before and after photo-induced cross-linking were studied using XRD spectra. As presented in Fig. 6a. Alg displayed diagnostic crys-

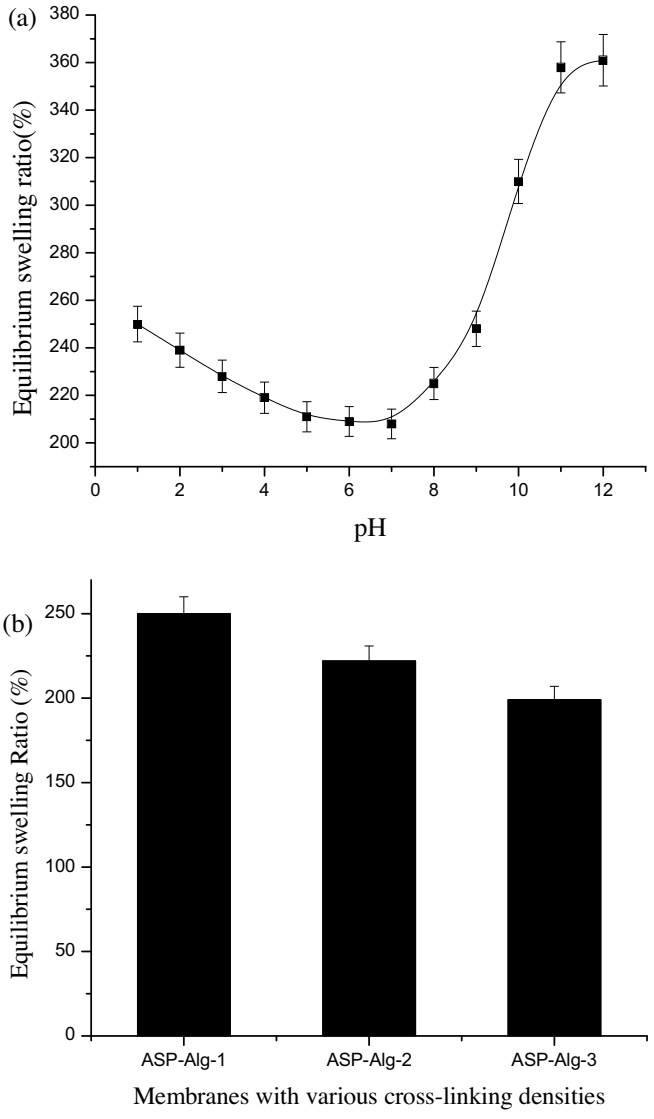

Fig. 8. (a) Swelling behaviors of photo-crosslinkedASP-Alg-2 hydrogel membrane as a function of pH (b) Swelling behaviors of different ASP-Alg hydrogel membranes with different cross-linking densities at pH 7.

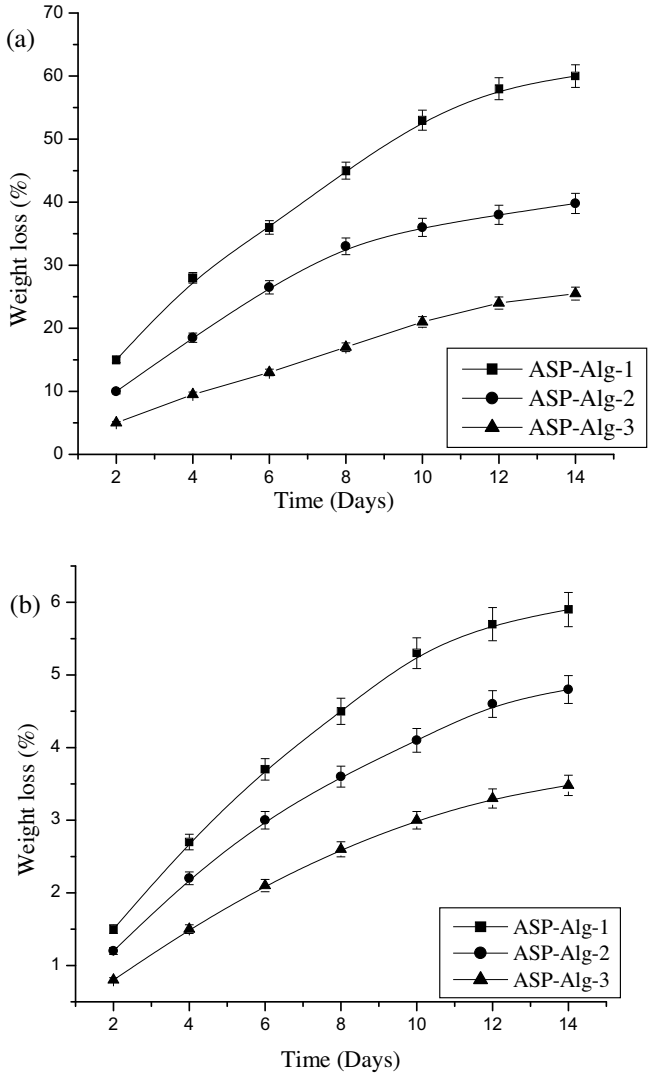

Fig. 9. In vitro biodegradation of the photo-crosslinked ASP-Alg hydrogel membranes incorporated with SBF under enzymatic conditions (a) and non-enzymatic conditions (b).

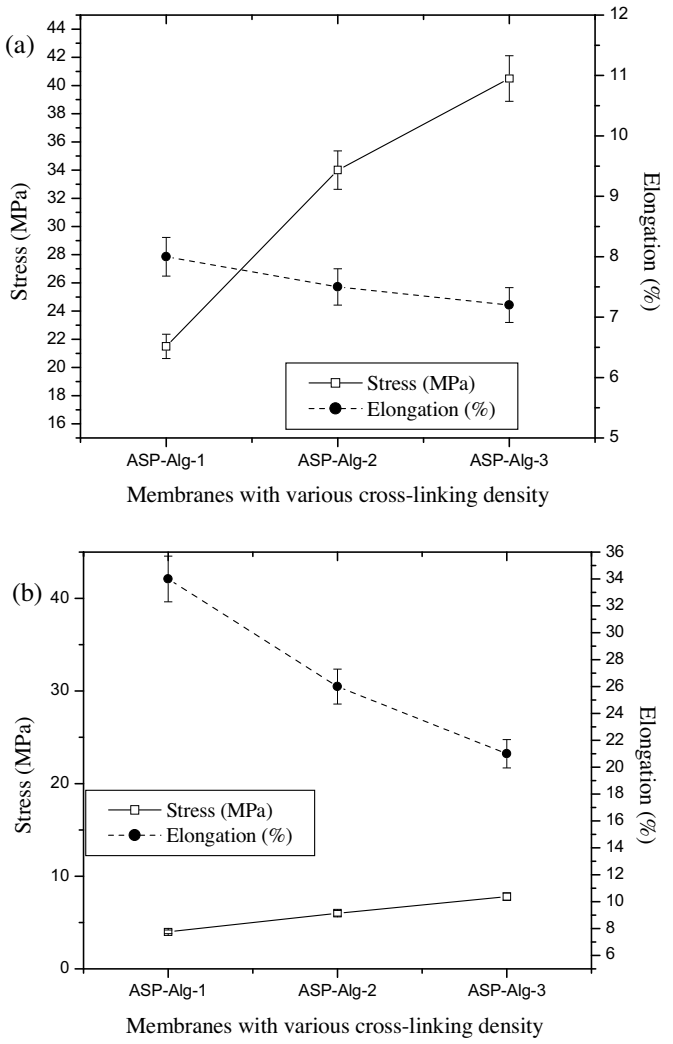

Fig. 10. Stress and elongation of ASP-Alg membranes under (a) dry conditionand (b) wet condition.

talline peaks at approximately 14.5°, 20.7° and 37.4°, which were in accordance with previous studies (Dong, Dong, Cao, Han, & Ding, 2011). After ASP modification, the spectrum of ASP-Alg-2 (Fig. 6b) exhibited a partial disappearance of these crystalline peaks indicating the reaction performance in the crystalline part as well as the amorphous part. Upon photo-crosslinking process, the crystalline peaks were completely disappeared (Fig. 6c) revealing the formation of mainly amorphous cross-linked network. This could be attributed to the cleavage of the hydrogen bonds that organize the crystalline structure of the polysaccharide chains.

The morphologies of the freeze–dried photo-crosslinked hydrogel membranes derived from ASP-Alg-1 and ASP-Alg-3 were visualized using SEM (Fig. 7). As can be noticed both samples presented a randomly distributed porous structure, however, the pore size exhibited an obvious decrease with increasing the degree of cross-linking, which reveal the potential application of these membranes in various biomedical fields such as drug delivery or enzyme immobilization.

3.4. Swelling behavior

The swelling behavior of the photo-crosslinked membrane derived from ASP-Alg-2 was studied as a function of pH value and the results were displayed in Fig. 8a. As can be seen, the hydrogel membrane exhibited medium swelling ratios under strong acidic condition, which was gradually decreased by increasing the pH up to 7, further increasing of pH was accompanied by a significant increase in the swelling ratio. This swelling behavior could be explained as in the following; under strong acidic medium, the inserted ASP units could be protonated and became positively charged, subsequently, the repulsion between these protonated moieties will increase the swelling by increasing the amount of absorbed water. On the other hand, in basic medium the carboxylate groups exist on the modified alginate backbone will be deprotonated and hence, the huge repulsion between the negatively charged polysaccharide chains will increase the swelling of the hydrogel. These were schematically presented in Scheme 3.

Moreover, at constant pH 7, the swelling of the hydrogel membranes was also examined as a function of the cross-linking degree. As shown in Fig. 8b, the swelling ratio displayed a significant lowering by increasing the degree of cross-linking. This of course could be related to the smaller pore size formed with higher cross-linking density.

Moreover, the obtained swelling ratio (%) values by the ASP-Alg are found to be competitive when compared to some other previously prepared alginate based hydrogel such as polyurethane grafted calcium alginate where the swelling degree was approxi-

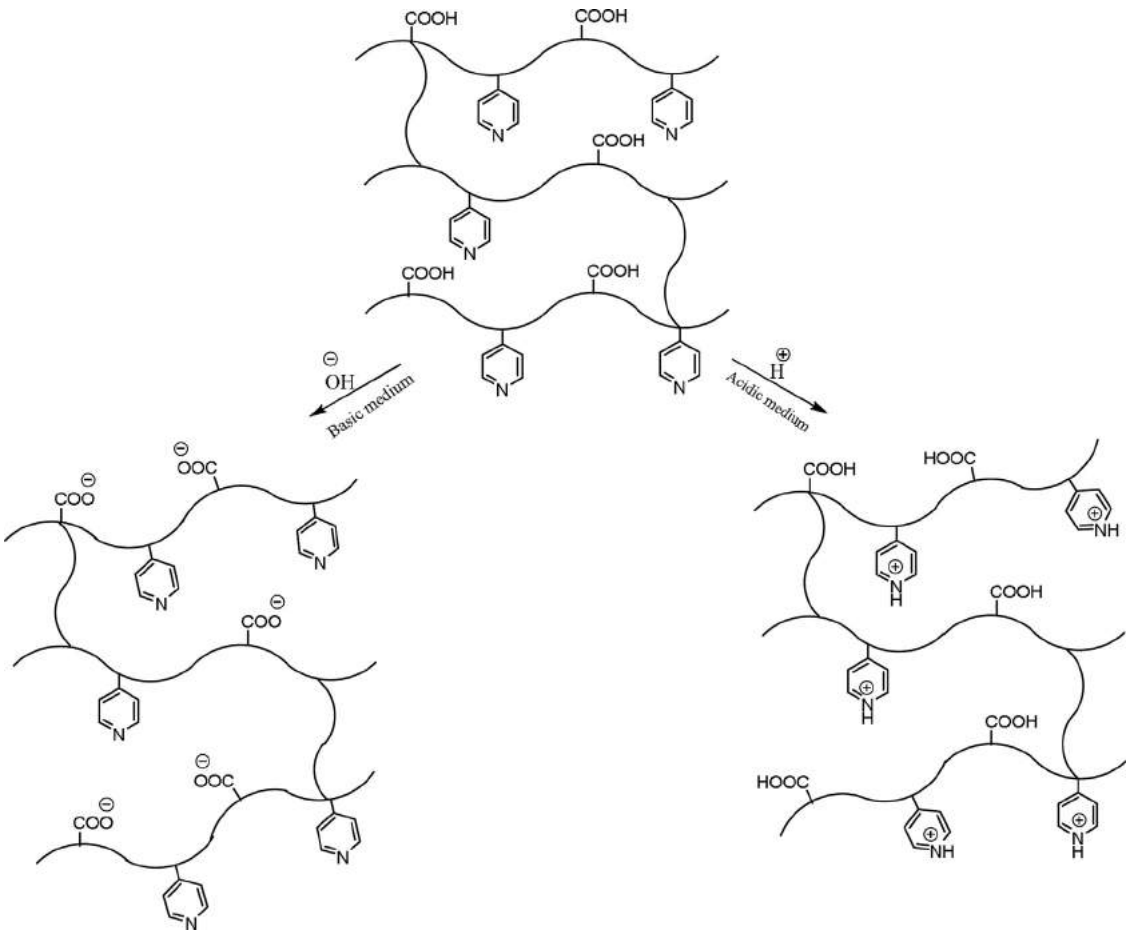

Scheme 3. Schematic presentation of photo-crosslinked ASP-Alg hydrogel membrane behavior under both acidic and basic medium.

mately 90% (Wang, Ying, Li, & Zhang, 2014), β-cyclodextrin/acrylic modified alginate hydrogel, which displayed about 80% swelling (Huang, Liu, Zhang, & Wu, 2014) and polyvinyl acetate grafted calcium alginate core-shell hydrogel microspheres where the swelling degree reached more than 300% (Ying, Qi, Li, Zhang, & Cheng, 2012).

3.5. In-vitro degradation

The in-vitro degradation under both enzymatic and non-enzymatic conditions had been carried out in order to anticipate the effect of the photo-crosslinking on the biocompatibility of the modified alginate membranes. The biodegradation was evaluated by estimating the weight loss (%) for both enzymatic and non-enzymatic conditions and the results are presented in Fig. 9. As expected, in presence of alginate lyase, the modified photo-crosslinked alginate membrane exhibited a rapid degradation rate compared to the non-enzymatic condition. However, the rate of the enzymatic degradation was significantly reduced by increasing the cross-linking density, within 14 days, the hydrogel membranes derived from ASP-Alg-1, ASP-Alg-2 and ASP-Alg-3 displayed approximate weight losses 58%, 35% and 25%, respectively. This of course could be attributed to the chemical alternations of the alginate structure, which will restrict the interaction with the enzyme and subsequently retard the degradation reaction.

Moreover, the hydrolytic degradation studies, which had been examined under non-enzymatic conditions (Fig. 9b) indicated that the studied hydrogel membranes almost maintained their structure integrity and resist the degradation in the whole duration of the study. After 14 days, the hydrogel samples displayed a comparatively small weight loss range 4.3–6.5%.

3.6. Mechanical properties

The mechanical properties of the manufactured membranes had been evaluated by examining the tensile strength and elongation as a function of cross-linking density under both dry and wet conditions. As presented in Fig. 10, the dry membranes (Fig. 10a) exhibited a significant increase in the tensile strength accompanied by an obvious lowering of the elongation by increasing the degree of cross-linking. This of course could be attributed to the common brittleness increase by increasing the cross-linking density (Monier, Wei, Sarhan, & Ayad, 2010). Furthermore, the wet membranes (Fig. 10b) displayed a similar trend; however, the tensile strength was obviously decreased while elongation was increased. This could be also explained as a result of the diffusion of the water molecules inside the cross-linked network, which behave like a plasticizer and increase the flexibility.

4. Conclusion

In this work we have presented the chemical modification of the natural polysaccharide alginate using photo-active 4-styryl-pyridine. The obtained photo-crosslinkable modified alginate (ASP-Alg) with various functionalization degrees were successfully investigated using elemental analysis, FTIR and NMR spectra. The photo-crosslinking process was performed upon UV irradiation through [2π + 2π] photo-chemical cycloaddition reaction,

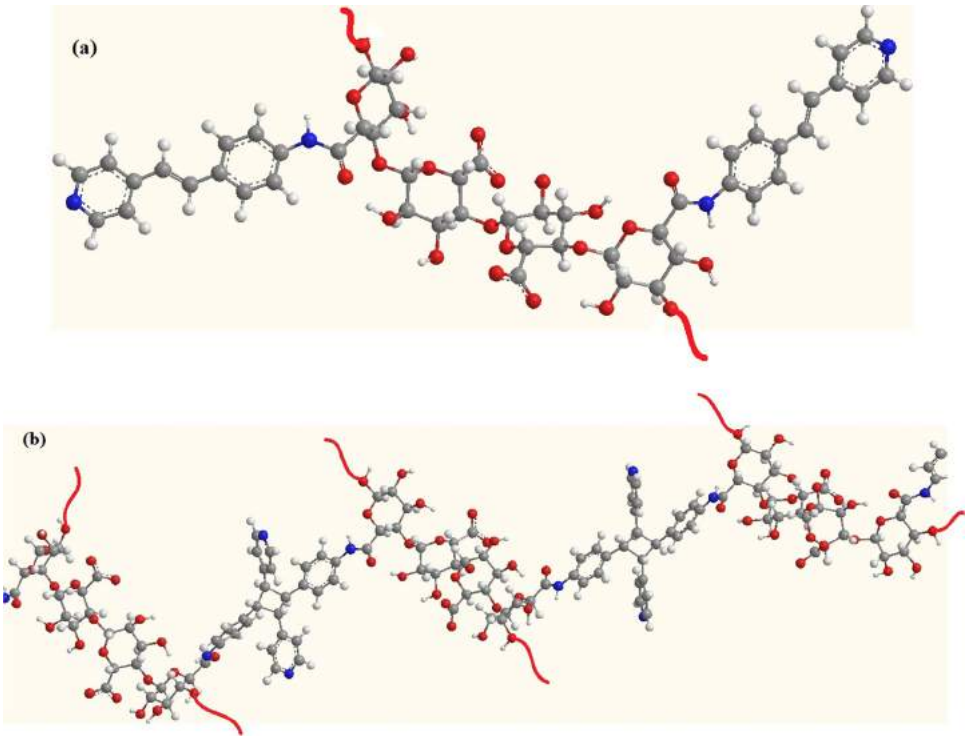

Structure 1. Molecular model of ASP-Alg (a) before photo-crosslinking and (b) after photo-crosslinking.

which was detected using UV–vis light spectra. Both crystalline and morphological structures of the obtained hydrogels with different crosslinking densities were examined utilizing XRD and SEM respectively. Moreover, the swelling behavior of the hydrogel displayed an obvious high swelling ratio (%) at high pH values and by lowering cross-linking density. Also, the biodegradability and mechanical properties revealed promising results for the possible application of the obtained photo-active materials such as drug delivery systems and enzyme immobilization.

Acknowledgement

The authors would like to acknowledge financial support for this work, from the King Abdulaziz City for Science and Technology (KACST) Saudi Arabia, under grant no. MS-35-0064. In addition, I would to acknowledge for University of Tabuk, Tabuk, Saudi Arabia.

References

Abd El-Ghaffar, M. A., & Hashem, M. S. (2013). Calcium alginate beads encapsulated PMMA-g-CS nano-particles for α-chymotrypsin immobilization. *Carbohydrate Polymers*, *92*, 2095–2102.

Abd Rahima, S. N., Sulaimana, A., Hamzah, F., Hamid, K. H. K., Rodhi, M. N. M., Musa, M., et al. (2013). Enzymes encapsulation within calcium alginate-clay beads: characterization and application for cassava slurry saccharification. *Procedia Engineering*, *68*, 411–417.

Agarwal, T., Gautham Hari Narayana, S. N., Pal, K., Pramanik, K., Giri, S., & Banerjee, I. (2015). Calcium alginate-carboxymethyl cellulose beads for colon-targeteddrug delivery. *International Journal of Biological Macromolecules*, *75*, 409–417.

Bruchet, M., & Melman, A. (2015). Fabrication of patterned calcium cross-linked alginate hydrogel filmsand coatings through reductive cation exchange. *Carbohydrate Polymers*, *131*, 57–64.

Bubenikova, S., Stancu, I.-C., Kalinovska, L., Schacht, E., Lippensc, E., Declercq, H., et al. (2012). Chemoselective cross-linking of alginate with thiol-terminated peptides for tissue engineering applications. *Carbohydrate Polymers*, *88*(2012), 1239–1250.

Castro, M. E., Percino, M. J., Chapela, V. M., Ceron, M., Soriano-Moro, G., Lopez-Cruz, J., et al. (2013). Theoretical and Experimental Spectroscopic Analysis of Cyano-Substituted Styrylpyridine Compounds. *International Journal of Molecular Sciences*, *14*, 4005–4029.

Chiang, C.-Y., & Chu, C.-C. (2015). Synthesis of photoresponsive hybrid alginate hydrogel withphoto-controlled release behavior. *Carbohydrate Polymers*, *119*, 18–25.

Daemi, H., & Barikani, M. (2012). Synthesis and characterization of calcium alginate nanoparticles, sodium homopolymannuronate salt and its calcium nanoparticles Scientia Iranica. *Transactions F: Nanotechnology*, *19*, 2023–2028.

De Santis, S., Diociaiuti, M., Cametti, C., & Masci, G. (2014). Hyaluronic acid and alginate covalent nanogels by template cross-linking in polyion complex micelle nanoreactors. *Carbohydrate Polymers*, *101*, 96–103.

Dong, Y., Dong, W., Cao, Y., Han, Z., & Ding, Z. (2011). Preparation and catalytic activity of Fe alginate gel beads for oxidative degradation of azo dyes under visible light irradiation. *Catalysis Today*, *175*, 346–355.

Dong, Y., Zhang, Y., Tu, B., & Miao, J. (2014). Immobilization of ammonia-oxidizing bacteria by calcium alginate. *Ecological Engineering*, *73*(2014), 809–814.

García-González, C. A., Alnaief, M., & Smirnova, I. (2011). Polysaccharide-basedaerogels-promising biodegradable carriers for drug delivery systems. *Carbohydrate Polymers*, *86*, 1425–1438.

Goh, C. H., Heng, P. W. S., & Chan, L. W. (2012). Alginates as useful natural polymerfor microencapsulation and therapeutic applications. *Carbohydrate Polymers*, *88*, 1–12.

Gong, R., Li, C., Zhu, S., Zhang, Y., Du, Y., & Jiang, J. (2011). A novel pH-sensitivehydrogel based on dual crosslinked alginate/N-_-glutaric acid chitosan for oraldelivery of protein. *Carbohydrate Polymers*, *85*, 869–874.

Graulus, G.-J., Mignon, A., Van Vlierberghe, S., Declercq, H., Fehér, K., Cornelissen, M., et al. (2015). Cross-linkable alginate-graft-gelatin copolymers for tissue engineering applications. *European Polymer Journal*.

Han, F., Dong, Y., Song, A., Yin, R., & Li, S. (2014). Alginate/chitosan based bi-layer composite membrane as potential sustained-release wound dressing containing ciprofloxacin hydrochloride. *Applied Surface Science*, *311*, 626–634.

Huang, Z., Liu, S., Zhang, B., & Wu, Q. (2014). Preparation and swelling behavior of a novel self-assembled β-cyclodextrin/acrylic acid/sodium alginate hydrogel. *Carbohydrate Polymers*, *113*, 430–437.

Jang, J., Seol, Y.-J., Kim, H. J., Kundu, J., Kim, S. W., & Cho, D. W. (2014). Effects of alginate hydrogel cross-linking density on mechanical and biological behaviors for tissue engineering. *Journal of The Mechanical Behavior of Biomedical Materials*, *37*, 69–77.

Laurienzo, P., Malinconico, M., Motta, A., & Vicinanza, A. (2005). Synthesis and characterization of a novel alginate–poly(ethylene glycol) graft copolymer. *Carbohydrate Polymers*, *62*(3), 274–282.

Lee, G.-S., Park, J.-H., Shin, U. S., & Kim, H.-W. (2011). Direct deposited porous scaffolds of calcium phosphate cement with alginate for drug delivery and bone tissue engineering. *Acta Biomaterialia*, *7*, 3178–3186.

Mandal, B., & Ray, S. K. (2013). Synthesis of interpenetrating network hydrogel from poly(acrylic acid-co-hydroxyethyl methacrylate) and sodium alginate: modeling and kinetics study for removal of synthetic dyes from water. *Carbohydrate Polymers*, *98*, 257–269.

Monier, M., Abdel-Latif, D. A., & Mohammed, H. A. (2015). Synthesis and characterization of uranyl ion-imprinted microspheresbased on amidoximated modified alginate. *International Journal of Biological Macromolecules*, *75*, 354–363.
Monier, M., Wei, Y., Sarhan, A. A., & Ayad, D. M. (2010). Synthesis and characterization of photo-crosslinkable hydrogel membranes based on modified chitosan. *Polymer*, *51*(2010), 1002–1009.
Nakamura, A., Irie, H., Hara, S., Sugawara, M., & Yamada, S. (2011). Photochemical & Photobiological. *Science*, *10*, 1496–1500.
Peng, C.-W., Lin, H.-Y., Wang, H.-W., & Wu, W.-W. (2012). The influence of operating parameters on the drug release and anti-bacterial performances of alginate wound dressings prepared by three-dimensional plotting. *Materials Science and Engineering C*, *32*, 2491–2500.
Pereira, R. F., Carvalho, A., Gil, M. H., Mendes, A., & Bártolo, P. J. (2013). Influence of Aloe vera on water absorption and enzymatic in vitrodegradation of alginate hydrogel films. *Carbohydrate Polymers*, *98*, 311–320.
Pluemsab, W., Sakairi, N., & Furuike, T. (2005). Synthesis and inclusion property of [alpha]-cyclodextrin-linked alginate. *Polymer*, *46*(23), 9778–9783.
Qiao, P., Wang, J., Xie, Q., Li, F., Dong, L., & Xu, T. (2013). Injectable calcium phosphate–alginate–chitosan microencapsulated MC3T3-E1 cell paste for bone tissue engineering in vivo. *Materials Science and Engineering C*, *33*, 4633–4639.
Stone, S. A., Gosavi, P., Athauda, T. J., & Ozer, R. R. (2013). In situ citric acid crosslinking of alginate/polyvinyl alcohol electrospun nanofibers. *Materials Letters*, *112*, 32–35.
Sweeney, I. R., Miraftab, M., & Collyer, G. (2014). Absorbent alginate fibres modified with hydrolysed chitosan forwound care dressings—II Pilot scale development. *Carbohydrate Polymers*, *102*, 920–927.
Tang, M., Chen, W., Weir, M. D., Thein-Han, W., & Xu, H. H. K. (2012). Human embryonic stem cell encapsulation in alginate microbeads in macroporous calcium phosphate cement for bone tissue engineering. *Acta Biomaterialia*, *8*, 3436–3445.
Tie, W., Zhong, Z., Li, L., Zhang, A., Shen, F., Lee, M.-H., et al. (2012). Synthesis and characterization of novel photosensitive polysulfones with photocrosslinkable side pendants. *European Polymer Journal*, *48*, 2070–2075.
Wang, J., Ying, X., Li, X., & Zhang, W. (2014). Preparation, characterization and swelling behaviors of polyurethane-grafted calcium alginate hydrogels. *Materials Letters*, *126*, 263–266.
Wang, Y., Chen, H., Wang, J., & Xing, L. (2014). Preparation of active corn peptides from zein through doubleenzymes immobilized with calcium alginate–chitosan beads. *Process Biochemistry*, *49*, 1682–1690.
Wu, J.-L., Wang, C.-Q., Zhuo, R.-X., & Cheng, S.-X. (2014). Multi-drug delivery system based on alginate/calcium carbonatehybrid nanoparticles for combination chemotherapy. *Colloids and Surfaces B: Biointerfaces*, *123*, 498–505.
Yang, L., Shi, J., Zhou, X., & Shaokui Cao, S. (2015). Hierarchically organization of biomineralized alginate beads for dualstimuli-responsive drug delivery. *International Journal of Biological Macromolecules*, *73*, 1–8.
Ying, X., Qi, L., Li, X., Zhang, W., & Cheng, G. (2012). Stimuli-responsive recognition of BSA-imprinted polyvinyl acetate grafted calcium alginate core-shell hydrogel microspheres. *Journal of Applied Polymer Science*, *127*, 3898–8909.
Zhu, C., Kustra, S. R., & Bettinger, C. J. (2013). Photocrosslinkable biodegradable elastomers based on cinnamate-functionalized polyesters. *ActaBiomaterialia*, *9*, 7362–7370.